Effects of Microstructural Variability on the Mechanical Properties of Ceramic Matrix Composites

M. B. GOLDSMITH, B. V. SANKAR, R. T. HAFTKA AND R. K. GOLDBERG

ABSTRACT

This paper presents a method to model variability in architectural parameters and predict the resultant uncertainty in the mechanical properties of a SiC/SiC ceramic matrix composite system. Using micrographs of three specimens, the relative importance of these architectural parameters on the mechanical properties is also identified. Both finite element analysis and an analytical method (Selective Averaging Method) are used. Response surfaces are used to relate the high-fidelity finite element analysis and the low-fidelity Selective Averaging Method. Various response surfaces are evaluated and used to obtain a large number of results in a relatively short amount of time (compared to using finite element analysis alone). The results reveal that modeling the random variation in all architectural parameters in a way that mimics the actual variation in the composite is important in order to obtain a satisfactory representation of the variability in the stiffness properties of the composite.

M.B. Goldsmith, Graduate Student (marlanab@ufl.edu)
B.V. Sankar, Ebaugh Professor (sankar@ufl.edu)
R.T. Haftka, Distinguished Professor (haftka@ufl.edu)
Department of Mechanical and Aerospace Engineering P.O. Box 116250, University of Florida, Gainesville, FL 32611, USA
R.K. Goldberg, Aerospace Engineer (Robert.goldberg@nasa.gov)
NASA Glenn Research Center, Mechanics and Life Prediction Branch, 21000 Brookpark Rd., Cleveland, OH 44135, USA

INTRODUCTION

Woven ceramic matrix composites (CMCs) such as SiC/SiC are candidate materials for future hypersonic vehicle systems such as thermal protection systems and aero-propulsion systems. Preliminary testing of these materials indicates that there is considerable variability in their thermal-mechanical properties such as Young's moduli and Poisson's ratios. One feature contributing to the properties' variability is the microstructural variability as discussed below. Hence it would be desirable to characterize the uncertainties. However, it is difficult to predict the variability in mechanical properties due to the architectural randomness in woven CMCs. The fabrication of these composites involves a complex multi-step process. The variability in the properties is due to uncertainties encountered at various stages of manufacturing, as well as variation within the constituents themselves [1,2]. Some of these uncertainties include constituent volume fractions, tow size, and tow spacing. In addition, due to the nature of the manufacturing, the SiC/SiC composite is known to have a large percentage of porosity that introduces further uncertainty [3].

Conventional design methodologies account for the aforementioned uncertainties by use of a safety factor, which may not allow a designer to take full advantage of the composite properties because the details of the microstructure are not rigorously accounted for. More recently other methods of accounting for the uncertainties have been explored. Some of these methods include a multi-level approach in which relationships are developed that link the lowest level (unidirectional composite) to the mid-level (woven composite), and finally to the highest level (laminated woven composite) [4]. While this approach may be effective in determining mechanical properties, it does not explicitly account for the effects of pore size, shape, and location along with other microstructural features which should not be neglected. The importance of accounting for these factors explicitly has recently been studied in a qualitative sense [5]. However, there is still a need to account for these factors in a quantitative sense. Additional analytical approaches accounting for certain details such as waviness or constituent volume fractions have also been developed, but again do not model porosity explicitly [6,7]. While these approaches may work very well for some woven composites, it is likely that they cannot adequately represent the SiC/SiC system.

Another approach is a nondeterministic approach in which uncertainties at the constituent level are used to determine the variability in mechanical properties. The advantage of probabilistic techniques is that they account for variation in a more realistic manner that may lead to a more efficient design. Such nondeterministic approaches require complete characterization of uncertainties in the composite. Thus there is a need to develop efficient methods to propagate the uncertainties from the primitive variables, e.g., fiber and matrix properties and porosity, to the response variables such as the stiffness of the composite material [8]. CMC's have been analyzed in a probabilistic manner in the past. However, this typically involved a "smearing" of the porosity into the matrix properties [2]. This assumption does not account for the size, shape, and the interaction of the voids with one another which can affect the mechanical properties. Additionally, variability in the microstructure was estimated, rather than rigorously quantified.

A methodology is presented for modeling the uncertainty in architectural parameters of a 5HS CVI (five harness satin weave, chemical vapor infiltrated) SiC/SiC composite, using micrographs of three specimens to identify the important parameters and their distributions. These are then used to perform Monte Carlo simulations of possible architectural variants. Analytical and finite element micromechanics simulations are then utilized to predict the scatter in mechanical properties. The Selective Averaging Method (SAM), an analytical method based on iso-stress and iso-strain assumptions, is used to analyze a large number of simulations that are corrected with a response surface based on the finite element results [9]. This is important because finite element analysis may not always be a feasible approach if a large number of samples are necessary to obtain an acceptable statistical representation of the results. A comparison is also made with a method in which no correction response surface (CRS) is used, but rather a linear high fidelity response surface of the finite element results. The uncertainty is parameterized based on measurable variables within the architecture to gain an understanding of the causes of variation in the mechanical properties. The results from this study are used to determine the sensitivity of response variables to several architectural parameters, as well as the expected distribution in mechanical properties due to these parameters.

ANALYSIS METHODS

Model Development and Description

The microstructure of the 5HS CVI SiC/SiC composite has been shown to have significant randomness. This results in high variability in the mechanical properties as well. A 2D image of one cross section of the composite, obtained by Bonacuse, et al. [10] is shown in Figure 1. The black area represents voids, which vary in location, size, and shape. Other 2D cross sections are not identical to the one shown, but rather, exhibit different random distributions of the voids and the microstructural characteristics such as tow size, shape, and spacing [10]. For this reason, it is difficult to define a representative volume element (RVE) that takes all of this variability into account. Therefore, some simplifying assumptions, explained in the following paragraphs, were made to develop an understanding of the composite at a basic level.

For this work, the focus was on modeling a RVE of the 5 HS composite rather than taking the lay-up of the composite into account, in order to keep the size of the problem tractable while developing the appropriate analysis methods. Hence, two architectural variations - ply shifting and tow nesting - that vary throughout the composite are not accounted for with the current RVE. Another feature that the current RVE does not capture is the non-uniform distribution of matrix. It is apparent in Figure 1 that the thickness of the matrix is much higher on the outside than on the inside of the composite. This is the nature of the current manufacturing process. All of these aspects that are currently being neglected will come into consideration in future work.

While there are a few architectural variations not captured by the current RVE, there is still a lot to learn from the parameters that are captured by the RVE used for

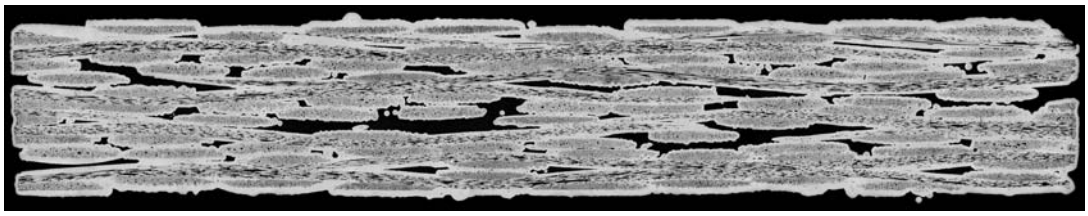

Figure 1: 2D cross section of the SiC/SiC composite microstructure

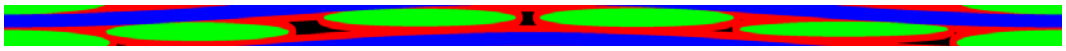

Figure 2: Example of a randomly generated RVE

this work and shown in Figure 2. Since this is a 5 HS weave, the RVE was defined as having five transverse tows that are aligned in such a way that they follow the sinusoidal curve of the longitudinal tow which runs continuously lengthwise across the cross section. This longitudinal tow, shown in blue, is held fixed for all analyses because there is currently no statistics available on its variation. The transverse tows, shown in green, are modeled as ellipses. The matrix, shown in red, is assumed to grow uniformly on the tows (the matrix thickness is the same on all tows, except where there is overlap) until a given matrix volume fraction is reached. This allows for the voids to be explicitly modeled in that the images seen are a result of the matrix growing on imperfectly sized and imperfectly aligned tows, which is a factor inherent in the production of voids.

Since the actual composite does continue “through the page” as it does in the longitudinal direction, a plane strain assumption is appropriate. It is important to note that it is assumed that every aspect of the 2D image is being extruded through the paper. Therefore, tow undulation and a closure of voids (rather than tunnels) is being neglected. For this reason, the modulus in the “through the page” direction is not accurate. It is expected that the true modulus will be more like that of the longitudinal direction.

Another important model characteristic to note is that the constituents are considered to be homogeneous. When percent void and percent matrix are being referred to, the porosity and the matrix volume fractions within the tow are not being accounted for. For example, the composite has a tow volume fraction of 60%. The tows, however, have their own fiber, matrix, and void volume fractions that are homogenized and referred to as the tow properties. It can be said then, that the volume fractions displayed represent inter-tow volume fractions.

In summary, the geometry and material properties of the transverse tows, the longitudinal tows, the matrix, and the voids, are all being explicitly modeled. The ply thickness is constant for every specimen. The selection of what parameters were chosen to be randomly varied is included in a later discussion.

Finite Element Analysis

The RVEs were generated as images (like that of Figure 2) with Python code, which were then meshed with the open source software, OOF2 [11]. OOF2 allows

the user to import an image and define the different materials by color selection. It then creates a mesh of a desired size with homogenous elements (each element has only one material associated with it). This mesh was then imported into commercial software, ABAQUS, for finite element analysis [12]. A combination of triangular and quadrilateral plane strain elements were used, to account for the in-plane thickness of the composite. An example of the mesh can be found in Figure 3. The material properties assigned were determined by Mital, et al. [13] and are shown in Table I. The yarn/matrix interphase is not explicitly modeled in the present study. The tows are modeled as homogenous but orthotropic materials, with resultant properties based on the fiber, matrix, pores, and interphase in the tows. The matrix is assumed to be an isotropic material.

In order to determine the effective elastic moduli and Poisson's ratios of the RVE based on the finite element analysis, the relationships in Equations 1 and 2 were used. This required three analyses for each specimen. Periodic boundary conditions were implemented for all analyses to simulate the repetition of the RVE [14]. The stiffness matrix [*C*] is found by first applying a finite strain, ε_1, and zero strain in the other two directions (ε_2 and ε_3). By volume averaging each of the three stresses (σ_1, σ_2, σ_3), the first column of the stiffness matrix is found. This is repeated in a similar manner for the second and third column. For the analysis to obtain the third column, generalized plane strain (rather than plane strain) elements were used so that a finite strain could be applied, rather than zero strain.

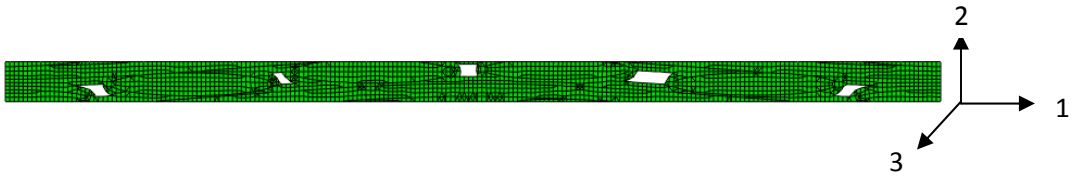

Figure 3: Example of finite element mesh of a RVE and coordinate system

TABLE I: CONSTIUENT MATERIAL PROPERTIES

	E_1 (GPa)	E_2 (GPa)	E_3 (GPa)	ν_{12}	ν_{13}	ν_{23}
Transverse Tow	106	106	259	0.21	0.21	0.18
Longitudinal Tow	259	106	106	0.18	0.21	0.21
Matrix	420	420	420	0.17	0.17	0.17

$$\begin{Bmatrix} \sigma_1 \\ \sigma_2 \\ \sigma_3 \end{Bmatrix} = \begin{bmatrix} C_{11} & C_{12} & C_{13} \\ C_{21} & C_{22} & C_{23} \\ C_{31} & C_{32} & C_{33} \end{bmatrix} \begin{Bmatrix} \varepsilon_1 \\ \varepsilon_2 \\ \varepsilon_3 \end{Bmatrix} \quad (1)$$

$$[C]^{-1} = \begin{bmatrix} S_{11} & S_{12} & S_{13} \\ S_{21} & S_{22} & S_{23} \\ S_{31} & S_{32} & S_{33} \end{bmatrix} = \begin{bmatrix} \begin{pmatrix} \frac{1}{E_1} & \frac{\nu_{21}}{E_2} & \frac{\nu_{31}}{E_3} \\ \frac{\nu_{12}}{E_1} & \frac{1}{E_2} & \frac{\nu_{32}}{E_3} \\ \frac{\nu_{13}}{E_1} & \frac{\nu_{23}}{E_2} & \frac{1}{E_3} \end{pmatrix} \end{bmatrix} \quad (2)$$

Selective Averaging Method

The Selective Averaging Method is an analytical method for determining elastic constants that was proposed by Sankar and Marrey [9]. The method simply requires a RVE and knowledge of the constituent material properties and their location. For this approach, the RVE is divided into slices. The slices are subdivided into elements. Then, the elastic constants of the constituents are averaged by selecting either the isostress or isostrain condition, depending on which is the more appropriate assumption for the given level being accounted for. For example, iso-strain is assumed when moving from the element level to the slice. This implies that every element within the slice has an equivalent strain. However, each slice can have a different strain. Then, from the slice to macroscale level, there is an isostress assumption in which every slice has an equivalent average stress. This method was shown to agree very well with FEA results for the 5HS weave that was used for comparison in their study. Further details can be found in Reference 9.

Response Surfaces

When it is desired to determine the response at a large number of data points, it is typical to perform analyses at a small set of data points, which are then fit with a polynomial response surface. The number of simulations needed is dependent on the number of variables, as well as the degree of the polynomial of your desired fit. Since all of the polynomials used in this work are linear, it is necessary to have at least one analysis per variable, plus one additional analysis for the constant term.

For this work, a linear high-fidelity (hi-fi) response surface, which will be referred to as LFERS (Linear Finite Element Response Surface) was used to generate a fit to the finite element analyses. An example of this equation is shown in Equation 3, where c is a constant and x is a chosen variable. Note that this equation and the ones following represent the response surface if only three variables are used. When the dependence of the response on the design variables is complicated, a higher order polynomial or another nonlinear equation may be required for the response surface. The number of coefficients may then be high, and the required number of simulations not computationally affordable. On the other hand, if a low-fidelity model captures well the nonlinear behavior, the total response may be captured by a simple correction to the low-fidelity model. In this case, Correction Response Surfaces (CRS) are used to combine less accurate and computationally inexpensive low fidelity (lo-fi) models, with more accurate (but computationally expensive) high fidelity (hi-fi) models. CRSs can allow for acceptable accuracy at a small computational cost. There are two commonly used

CRSs. One is the multiplicative CRS (in which a ratio between the hi-fi and lo-fi analyses is used). It is only computationally affordable for this problem to use a linear CRS. This method will be referred to as the linear multiplicative CRS (LMCRS), and an example is shown in Equation 4. The other CRS is a linear low to high fidelity response surface (in which a CRS is made with the linear relationship between hi-fi and lo-fi results), and is shown in Equation 5. Note that the LCRS method does not explicitly account for the design variables, and therefore the number of constants in the equation does not change with the number of variables.

$$hi-fi\ results = c_1 * x_1 + c_2 * x_2 + c_3 * x_3 + c_4 \tag{3}$$

$$\frac{hi-fi\ results}{lo-fi\ results} = c_1 * x_1 + c_2 * x_2 + c_3 * x_3 + c_4 \tag{4}$$

$$hi-fi\ results = c_1 * (lo-fi\ results) + c_2 \tag{5}$$

In the current work, 15 random variables were chosen as explained in the section to follow. For a linear response surface in 15 variables, a minimum of 16 high fidelity models are necessary (one analysis for each constant). Thirty-two models were used for improved accuracy. For the selection of the variable values of the 32 FEA models, Latin Hypercube Sampling was used. This technique ensures representation of a realistic variability by generating non-repetitive samples that are evenly distributed in the design space. The computational burden for this number of high-fidelity analysis is high, creating a necessity for a low-fidelity analysis method. For the low fidelity SAM analysis, 1,000 models were analyzed. This number was chosen because with 1,000 samples and an expected standard deviation that is 10% of the mean, it is predicted that the mean and standard deviation will have an error of order 0.3 percent and 3.0%, respectively(the error are approximately the standard deviation divided by the square root of the number of samples).

Selection of Variables and Statistics

The parameters chosen to be randomly varied were selected based on whether or not statistical data was currently available for those parameters. It was desired to only randomize the parameters that had quantifiable randomness, with as little guess work involved as possible. The geometric parameters in which statistical data was available were transverse tow width (*w*), transverse tow height (*h)*, and transverse tow spacing in the longitudinal direction (*s*). See Figure 4 for the definition of these variables within a RVE. Other architectural parameters, such as tow spacing in the through thickness ("2") direction and longitudinal tow amplitude (the difference between the maximum and minimum height of the longitudinal tow) are either dependent on the variables used, or were approximated based on visually fitting the geometry to the specimens. The variables that do not yet have statistical data were held constant. An issue that further complicates the problem is that the variables not only vary between the specimens, but they have a variation within each specimen as well. Therefore, each transverse tow is assigned an individual, but

correlated tow width, tow height, and tow spacing. Since there are five tows in the RVE, this results in a total of fifteen variables (five tow widths, five tow heights, and five tow spacings).

The random generation of the fifteen variables was based on the statistical data in three different specimens for which micrographs were available (similar to the one shown in Figure 1). Every tow width, tow height, and tow spacing were made available through image processing techniques [10]. Since it was desired to only model one 2D RVE of the composite (five transverse tows for a 5HS weave), the statistics were taken from the first five complete tows in each of the eight plies for each of the three specimens. The segment bounded in Figure 5 is an example of approximately where in the composite the statistics came from. This means that for each of the five tows, there were twenty-four data points to base the statistical distributions on (a total then, of 120 points). It was found from the 120 measures that the tow spacing and tow width had a normal distribution while the tow height had a Weibull distribution. These distributions were accounted for when generating random variables for each RVE.

In addition to determining the type of distribution associated with these parameters, it was found that there was meaningful correlation between the tow spacing and tow width for each variable. For this reason, correlation coefficients were accounted for during the generation of variables. For calculation of correlation coefficients, 24 measurements could be used for each of the fifteen variables. Making use of correlation parameters ensured that inherent architecture variation due to the manufacturing process would be accounted for and the generation of unrealistic specimens would be minimized.

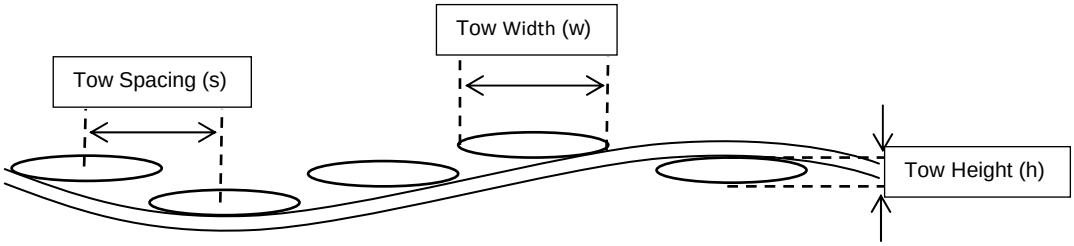

Figure 4: Definition of the tow spacing, tow width, and tow height

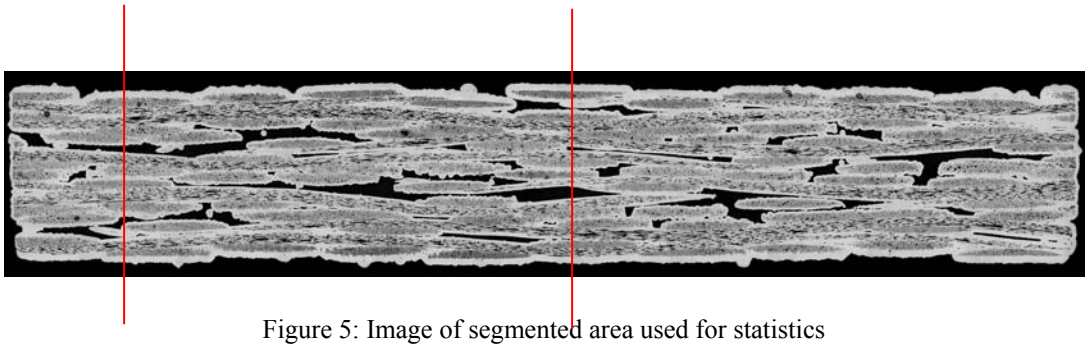

Figure 5: Image of segmented area used for statistics

RESULTS AND DISCUSSION

The discussion below presents a comparison of how well aspects of the artificially generated models based on statistics compare to the actual specimens. Then, the results from the finite element analysis and the analytical method combined with the response surfaces are discussed.

Comparison of Real Specimens to Artificially Generated Specimens

A summary of the characteristics of the specimens generated for the three sample specimens from which the statistics were obtained is presented in Table II. Comparisons can be drawn between these characteristics, and those of the artificially generated parameters summarized in Tables III and IV. The most obvious aspect to point out is that the volume fractions for the voids are significantly different. This discrepancy was expected and is due to not accounting for imperfections in alignment of the plies (ply shifting). The tow volume fractions therefore increase slightly to compensate for this loss in void volume fraction. In addition, the distribution of matrix is not uniform in the actual composite which could be another cause of the lower void volume fraction in the artificially generated specimens [13]. However, the standard deviations remain close to those of the three specimens.

The architectural aspects compare better than the volume fractions. This is expected since the randomization was based on the statistics of the architectural parameters listed. The means and standard deviations compare exactly up to the third significant digit. However, the range of values explored in the artificial data is larger than that of the actual specimens. If statistics are taken from additional actual specimens, it is expected that the range of values will increase to more closely match that of the artificially generated specimens. Histograms that give a visual representation of the distribution of variables for the 1,000 specimens are shown in Figure 6. A normal distribution in red is shown on top of the histogram for reference. It is apparent that the tow width and tow spacing follow a normal distribution, while the tow height is closer to a Weibull distribution, as was designated while generating the variables.

The correlation coefficients for the artificial and generated data were also compared. A few of the significantly correlated parameters (correlation parameter is great than 0.3) are as follows. Spacing three (the spacing between the third and fourth tow) was highly correlated to all of the others spacings with the exception of the final spacing. The second spacing was highly correlated to all of the tow widths that followed in sequence. The final two spacings are highly correlated as well. It was found that out of the twelve correlations parameters deemed significant, only two had notable errors of 10% and 13%. The rest of the errors associated with significant correlation coefficients were below 10%. It is likely that the spacing and width have some degree of correlation because when the composites are manufactured they are restricted to a certain width. Therefore, depending on the tow sizes, the spacing has to adjust to accommodate for all of the tows. The good agreement between artificially generated data and that of the actual data is due to the proper statistical distribution being accounted for, as well as the correlation coefficients.

TABLE II: SUMMARY OF VOLUME FRACTION AND GEOMETRIC CHARACTERISTICS FOR 3 REAL SAMPLE SPECIMENS

	% Void	% Matrix	% Tow	w (mm)	s (mm)	h (mm)
Max Value	8.70	33.80	60.80	1.31	1.33	0.16
Min Value	6.90	32.30	57.50	0.88	1.11	0.09
Range	1.80	1.50	3.30	0.43	0.22	0.07
Mean Value	8.03	32.83	59.13	1.07	1.22	0.12
St. Dev.	0.99	0.84	1.65	0.08	0.05	0.02

TABLE III: SUMMARY OF VOLUME FRACTION AND GEOMETRIC CHARACTERISTICS FOR 32 SPECIMENS

	% Void	% Matrix	% Tow	w (mm)	s (mm)	h (mm)
Max Value	4.29	31.58	71.10	1.30	1.41	0.17
Min Value	1.33	27.13	66.31	0.78	1.06	0.08
Range	2.96	4.45	4.79	0.52	0.34	0.09
Mean Value	2.75	29.17	68.08	1.07	1.22	0.12
St. Dev.	0.69	1.05	1.13	0.08	0.05	0.02

TABLE IV: SUMMARY OF VOLUME FRACTION AND GEOMETRIC CHARACTERISTICS FOR 1000 SPECIMENS

	% Void	% Matrix	% Tow	w (mm)	s (mm)	h (mm)
Max Value	6.34	34.17	75.81	1.43	1.42	0.19
Min Value	0.02	24.17	60.40	0.75	1.04	0.09
Range	6.32	10.00	15.41	0.67	0.38	0.10
Mean Value	2.91	29.28	67.81	1.07	1.22	0.12
St. Dev.	1.17	1.64	2.51	0.08	0.05	0.02

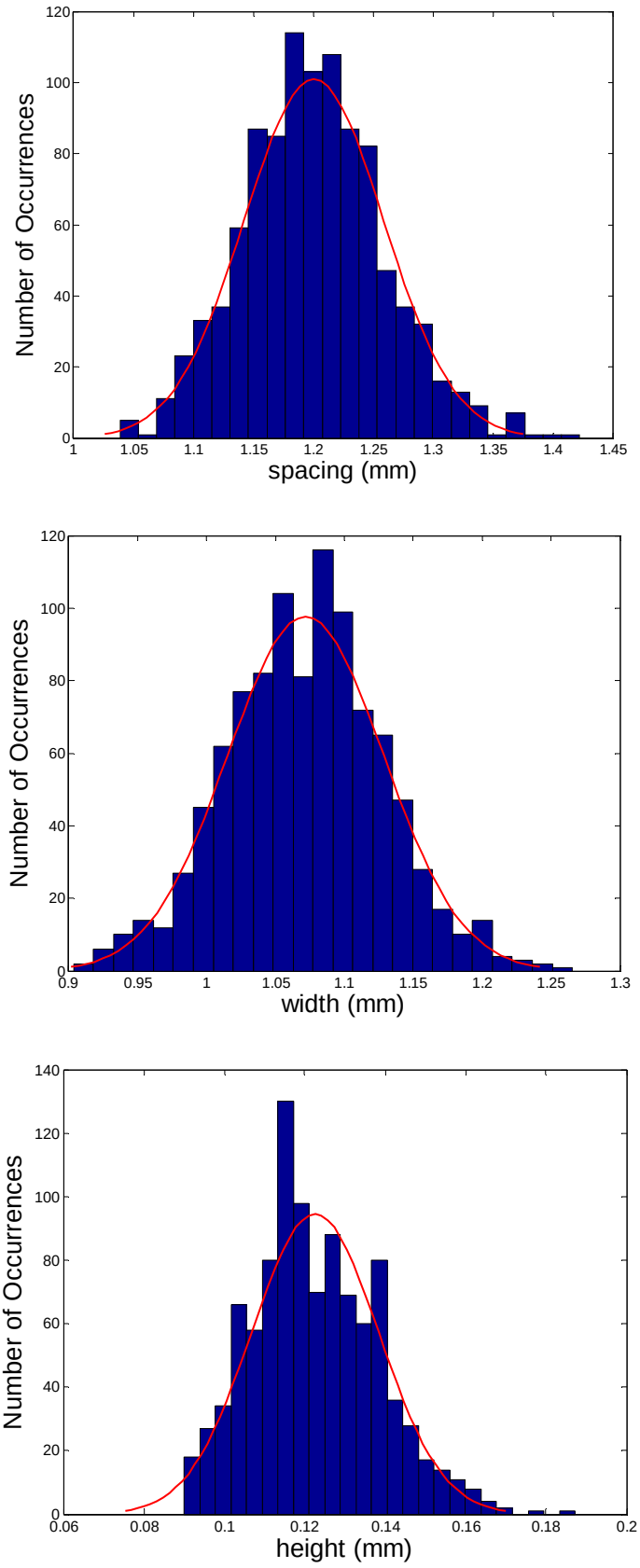

Figure 6: Histograms of the distribution of the variables for 1,000 specimens

FEA, SAM, and Response Surfaces

It was hypothesized that the best method to obtain accurate results at a low computational cost would be through the use of a correction response surface. The ratio between the response variables with FEA and SAM analysis was fairly consistent (the standard deviation was less than two percent of the mean) so it was hypothesized that fitting the ratio between the results of the two methods (LMCRS) would give the most desirable results. Two other methods were also used for comparison. One of those is the linear low to high fidelity response surface in which a linear fit was made from the SAM results to the FEA results (LCRS), with no geometric parameters taken into account explicitly. The final method was the linear high fidelity response surface, in which a response surface is fit to the FEA data only (LFERS). It was found that there was no valuable information gained from the implementation of the LCRS. Therefore, the discussion will be limited to the results from the LMCRS and LFERS.

The coefficients in the response surface associated with each variable for the LMCRS and LFERS are displayed in Tables V and VI, respectively. They are the response surface coefficients multiplied by the range for the variable associated with them in order to account for the fact that some of the variables have different dimensions. The statistically significant coefficients (as measured by the t-statistic) are marked with an asterisk. An important aspect of these tables to note is that the response surface includes two additional variables that were not previously mentioned, matrix volume fraction (MVF) and tow volume fraction (TVF). Void volume fraction is not included because the coefficient associated with it is accounted for by the matrix and void volume fractions, since the sum of the volume fractions will always be one. Initially, the response surfaces were fit to only the 15 variables that were manually being varied. However, the accuracy of the correction response surface was not satisfactory, and it was the found that the inclusion of volume fractions reduced the standard error substantially (by a factor of four). Even though the volume fractions are not explicitly varied as the architectural parameters are, it is obvious that the changes in the volume fraction significantly affect the mechanical properties in a way that is not accounted for by the architectural parameters alone, especially for the LMCRS.

For the LMCRS, the matrix volume fraction plays the largest role in the determination of all of the moduli as seen in Table V. It is especially prominent for the in-plane moduli. The tow volume fraction is also significant for the moduli. However, the Poisson's ratios depend less on the matrix volume fraction than the moduli, and more on the tow volume fraction. The dependence on the architectural parameters can also be extracted. The tow spacing and height is rather important for E_1 as compared to the width. However, the other mechanical properties are more uniformly dependent on transverse tow height, width, and spacing.

The results in Table VI reveal that for the FERS, the matrix and tow volume fractions are still important, but less so. This is likely due to the fact that in the calculations involved with SAM constituent properties are integrated to determine mechanical properties. Therefore, how much there is of each constituent is important. In other words, the architectural parameters influence the volume fractions, but the volume fractions ultimately influence the mechanical properties. When using the FERS surface, results from SAM are not used, and hence the

dependence on volume fractions has less of an influence. Instead, the physical interactions between constituents' size, shape, and spacing are being accounted for. The dependence on architectural parameters for both cases, however, is similar. The tow spacing and tow height remain the most important factors in the determination of E_1. The dependence on architectural parameters for other mechanical properties is more even distributed.

The importance of including all architectural parameters is further highlighted in Table VII. Another way in which the effect of the variables was investigated was to first generate 1,000 more specimens to be solved analytically. The new specimens, however, would fix the tow height at the average value, and only vary the tow spacing and tow width (leaving 10 variables). Correlation was still accounted for in the parameters that were not fixed. This was repeated two more times fixing the tow width and the tow spacing at their respective values. While the mechanical properties calculated through the analytical method contain some errors, the range of values can still serve as a basis of comparison. The percent difference in the maximum and minimum values for the response variables for the original 1,000 cases when all fifteen variables were present are compared to the percent difference in the maximum and minimum values when a certain variable was fixed in Table VII. For example, the second column displays the percent difference in range of values calculated when height was held constant, while width and spacing were still allowed to vary. It becomes clear that randomizing all variables is important to get an acceptable range of values, but the transverse tow height is especially important. When tow height is given a uniform value, the range of values significantly decreases for all three response variables. The information in the table implies that it is important to account for the variation due to all fifteen random variables.

Before analyzing the results, it is important to understand the quality of the response surfaces. To do so, cross validation was completed. Cross validation removes one point from the 32 analyses, and calculates a response surface based on the 31 remaining data points. It then calculates the result for the point removed based on the response surface, and compares that value to what this known point should have been. The calculations were done using a Surrogates Toolbox programmed for MATLAB [16]. The results for cross validation are shown in Table VIII. The first row is the cross validation errors when volume fractions (VFs) are not used and the second row is the cross validation errors when volume fractions are used. It is clear that using the volume fractions is important to obtaining a good quality fit for the LMCRS, which agrees with observations made from Table V. Even though the quality of the LMCRS improved, there is still a substantial error for E_2.

Table VIII also reveals that for some mechanical properties, the quality of the FERS actually decreases with the addition of volume fractions. Again, this is likely due to the fact that the dependence on volume fraction is more inter-related to the architectural parameters for FEA than it is for SAM. It's possible that for the LMCRS, volume fractions must be included, while for FERS it may not be necessary.

Another way in which the quality of the response surfaces was checked was to choose three specimens from the 1,000 generated specimens and analyze them using the finite element analysis. The results were then compared to those of the

output according to various response surfaces. The three specimens were chosen such that one had the smallest void volume fraction (specimen 453, approximately 0.02%), one had the largest void volume fraction (specimen 660, approximately 6%), and one had a void volume fraction near the average (specimen 979, approximately 3%). The errors found when comparing each of the three response surface methods to the actual finite element results are summarized in Tables IX through XI. The corresponding illustrations of each specimen are shown in Figures 7 through 9. A few of the errors associated with comparing the calculations according to the response surfaces to the FEA analysis are higher than desirable. Both the FERS and LMCRS have errors associated with them in such a way that makes it difficult to conclude whether or not one response surface is better than the other, especially since only three specimens are being compared.

TABLE V: COEFFICIENTS BASED ON THE LMCRS

	E_1	E_2	E_3	ν_{12}	ν_{13}	ν_{23}
w_1	-18	23	-36*	30	15	64
w_2	-7	47*	-31*	-66*	44*	59*
w_3	-3	34	-8	-46	34*	33
w_4	-13	43*	-27*	-76*	44*	60*
w_5	-2	35	-24*	-3	22	72*
s_1	-43*	-41	-24*	68*	-33*	-35
s_2	-49*	-64*	-19	91*	-45*	-48
s_3	-40*	-4	-32*	43	-24*	7
s_4	-45*	-42*	-17*	33	-25*	-35
s_5	-27*	-27	-16*	-3	-13	-31
h_1	-34*	72*	-22*	-67*	52*	89*
h_2	-33*	22	-21*	64*	18	60*
h_3	-52*	39	-25*	-11	37*	67*
h_4	-44*	62*	-37*	-30	35*	109*
h_5	-55*	30	-31*	17	27	69*
MVF	-125*	-86*	-79*	-0.2	0.3	-3
TVF	-39*	-63*	-53*	48*	-32*	-27

TABLE VI: COEFFICIENTS BASED ON THE FERS

	E_1	E_2	E_3	ν_{12}	ν_{13}	ν_{23}
w_1	-66*	83	-91*	10	33	122
w_2	-33*	90*	-80*	-127*	85*	108*
w_3	-30	26	-22	-57	64*	53
w_4	-9	81*	-69*	-129*	82*	115*
w_5	-6	85	-65*	-21	44	140*
s_1	-113*	-111*	-66*	152*	-67*	-70
s_2	-121*	-120	-49	162*	-87*	-91
s_3	-86*	-46	-86*	120*	-53*	6
s_4	-81*	-110*	-44*	102*	-54*	-66
s_5	-61*	-65	-41*	11	-27	-57
h_1	-92*	116*	-59*	-107*	100*	161*
h_2	-98*	50	-56*	102*	37	114*
h_3	-136*	69	-65*	-20	71*	122*
h_4	-93*	130*	-95*	-63	69*	205*
h_5	-147*	63	-82*	21	52	128*
MVF	-57*	-5	-13	-11	-21	-1
TVF	-54*	-37	-1	50	-47*	-32

TABLE VII: PERCENT DIFFERENCE IN RANGE OF MAXIMUM AND MINIMUM VALUES ACCORDING TO SAM WHEN ALLOWING ALL 15 VARIABLES TO HAVE A RANDOM DISTRIBUTION VERSUS HOLDING SELECTED VARIABLES CONSTANT

	Original	**Uniform Height**	**Uniform Width**	**Uniform Spacing**
E_1	14.4	1.64	14.53	18.11
E_2	13.95	3.43	11.49	15.33
E_3	7.13	5.23	3.41	6.47

TABLE VIII: CROSS VALIDATION PERCENT ERRORS FOR RESONSE SURFACES

	E_1		E_2		E_3	
	FERS	LMCRS	FERS	LMCRS	FERS	LMCRS
VFs NOT included in Response Surface	0.52	2.7	1.9	2.2	0.37	1.3
VFs included in Response Surface	0.46	0.7	2.1	1.6	0.45	0.48

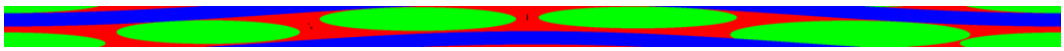

Figure 7: Specimen 453

TABLE IX: SPECIMEN 453, SUMMARY OF RESULTS FOR RESPONSE SURFACES

	E_1 (GPa)	E_2 (GPa)	E_3 (GPa)	ν_{12}	ν_{13}	ν_{23}
FEA	219	136	245	0.195	0.196	0.175
LMCRS	226	136	241	0.221	0.193	0.181
% Error	-3.19	0.29	1.83	-13.09	1.30	-3.16
LFERS	218	144	240	0.211	0.195	0.182
% Error	0.44	-5.64	1.85	-8.19	0.47	-3.89

Figure 8: Specimen 660

TABLE X: SPECIMEN 660, SUMMARY OF RESULTS FOR RESPONSE SURFACES

	E_1 (GPa)	E_2 (GPa)	E_3 (GPa)	ν_{12}	ν_{13}	ν_{23}
FEA	241	120	268	0.214	0.179	0.140
LMCRS	246	133	265	0.199	0.185	0.148
% Error	-2.25	-10.74	0.99	6.88	-3.25	-5.53
LFERS	248	129	266	0.203	0.185	0.147
% Error	-3.09	-7.88	0.83	5.05	-3.25	-4.87

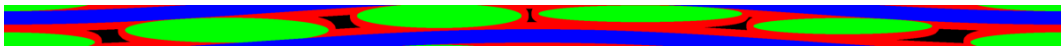

Figure 9: Specimen 979

TABLE XI: SPECIMEN 979, SUMMARY OF RESULTS FOR RESPONSE SURFACES

	E_1 (GPa)	E_2 (GPa)	E_3 (GPa)	ν_{12}	ν_{13}	ν_{23}
FEA	237	126	257	0.204	0.185	0.149
LMCRS	237	125	257	0.207	0.185	0.147
% Error	-0.09	0.82	0.07	-1.40	0.09	1.56
LFERS	238	125	257	0.207	0.185	0.147
% Error	-0.35	0.67	0.04	-1.48	0.09	1.35

Mechanical Properties

A summary of the mechanical properties calculated with different methods are shown below in Tables XII through XVII. The mean values of the mechanical properties for various methods agree fairly well with one another, with the exception of E_2 and ν_{23}. The reason for this discrepancy is currently being investigated. The analytical method (SAM) accounts for voids by simply assigning the void area negligibly small mechanical properties. It is possible that unlike the finite element method, the effects of interaction between voids, and the effects of their size and shape are not being accounted for. This could highlight voids' structural effects, which goes beyond "knocking down" constituent properties as has been done in the past. The discrepancy between values calculated with two different methods is an aspect that is ideally accounted for by a CRS. It should also be noted that it is not surprising for E_2 to be significantly lower than the other elastic moduli. The highest variations in mechanical properties occur with E_2 and ν_{23}. These are similar effects that were seen in finite element results of full specimens, as well as in studies completed by others for voids in unidirectional fiber reinforced composites [5,15]. The standard deviations are slightly higher for the results with 1,000 analyses because there are more specimens generated, resulting in the variables themselves having a slightly larger range (as seen earlier in Tables III and IV). The standard deviation for the FERS is not as close to the

original standard deviations as the LMCRS, which is likely because of the error in the fit.

TABLE XII: SUMMARY OF E_1 SOLVED WITH VARIOUS METHODS

	32 FEA	32 with FERS	32 SAM corrected with LMCRS	1000 SAM Uncorrected	1000 FERS	1000 SAM Corrected with LMCRS
Mean (GPa)	236.8	236.8	236.8	239.2	238.2	238.2
St. Dev. (GPa)	4.3	4.3	4.3	6.0	7.9	6.2
Max (GPa)	245.2	245.0	244.7	257.0	266.5	260.6
Min (GPa)	225.4	225.1	225.0	220.0	214.5	218.8
Range (GPa)	19.8	19.9	19.7	37.0	52.0	41.8

TABLE XIII: SUMMARY OF E_2 SOLVED WITH VARIOUS METHODS

	32 FEA	32 with FERS	32 SAM corrected with LMCRS	1000 SAM Uncorrected	1000 FERS	1000 SAM Corrected with LMCRS
Mean (GPa)	130.6	130.6	130.6	187.8	130.5	130.5
St. Dev. (GPa)	3.9	3.6	3.7	4.3	4.8	4.4
Max (GPa)	138.2	137.3	138.3	202.0	144.6	144.1
Min (GPa)	123.2	123.2	123.6	173.8	113.5	116
Range (GPa)	15.0	14.1	14.7	28.2	31.1	28.1

TABLE XIV: SUMMARY OF E_3 SOLVED WITH VARIOUS METHODS

	32 FEA	32 with FERS	32 SAM corrected with LMCRS	1000 SAM Uncorrected	1000 FERS	1000 SAM Corrected with LMCRS
Mean (GPa)	256.8	256.8	256.8	259.0	257.1	257.1
St. Dev. (GPa)	3.6	3.5	3.5	2.7	5.5	5.5
Max (GPa)	266.3	265.2	265.1	268.7	279	278.6
Min (GPa)	249.2	249.6	249.7	249.5	240.5	240.5
Range (GPa)	17.1	15.6	15.4	19.2	38.5	38.1

TABLE XV: SUMMARY OF ν_{12} SOLVED WITH VARIOUS METHODS

	32 FEA	32 with FERS	32 SAM corrected with LMCRS	1000 SAM Uncorrected	1000 FERS	1000 SAM Corrected with LMCRS
Mean	0.206	0.206	0.206	0.182	0.205	0.205
St. Dev.	0.004	0.004	0.004	0.001	0.005	0.006
Max	0.214	0.214	0.214	0.185	0.219	0.228
Min	0.197	0.197	0.197	0.179	0.191	0.184
Range (GPa)	0.017	0.017	0.017	0.006	0.029	0.044

TABLE XVI: SUMMARY OF ν_{13} SOLVED WITH VARIOUS METHODS

	32 FEA	32 with FERS	32 SAM corrected with LMCRS	1000 SAM Uncorrected	1000 FERS	1000 SAM Corrected with LMCRS
Mean	0.187	0.187	0.187	0.194	0.187	0.186
St. Dev.	0.003	0.003	0.003	0.001	0.003	0.003
Max	0.192	0.192	0.192	0.198	0.196	0.195
Min	0.182	0.181	0.181	0.189	0.175	0.176
Range (GPa)	0.010	0.010	0.010	0.008	0.021	0.019

TABLE XVII: SUMMARY OF ν_{23} SOLVED WITH VARIOUS METHODS

	32 FEA	32 with FERS	32 SAM corrected with LMCRS	1000 SAM Uncorrected	1000 FERS	1000 SAM Corrected with LMCRS
Mean	0.155	0.155	0.155	0.184	0.155	0.155
St. Dev.	0.006	0.005	0.005	0.001	0.008	0.008
Max	0.167	0.167	0.167	0.187	0.182	0.181
Min	0.142	0.143	0.143	0.182	0.129	0.130
Range (GPa)	0.025	0.024	0.024	0.004	0.053	0.051

CONCLUSIONS

The goal of this work was to select an RVE with architectural parameters that could be varied to effectively represent the variation in the SiC/SiC composite, and develop a method in which the variability in mechanical properties could be predicted in a computationally efficient manner, while also gaining an understanding of what geometric parameters were influential in determining the mechanical properties. The method of artificially generating specimens by using statistical information from the micrographs of actual composite specimens works very well. The statistics of the real and artificially generated specimens are in agreement. In addition, the mechanical properties calculated for the real specimens and the artificially generated specimens do not differ greatly.

In regards to determining the response surfaces, it was also found that in some cases, even if the volume fractions aren't explicitly varied, it is still important to include their inherent variation in the correction response surface. While the uncertainty associated with the calculation of the mechanical properties could be reduced with an improvement in the response surface quality, it is clear that it is important to model the randomness of all of the variables used in this paper (and likely some additional ones) in order to capture a realistic and fully representative variation in mechanical properties.

ACKNOWLEDGMENTS

The funding for this work was provided by the NASA Graduate Student Research Program, grant number NNX10AM49H. The authors are thankful to Kim Bey of NASA LaRC for many helpful discussions. Also, thanks to Pete Bonacuse of NASA GRC for the code for model generation as well as the parameter sample

distributions, and to Subodh Mital of The University of Toledo and NASA GRC for helpful discussions regarding finite element modeling and OOF2.

REFERENCES

1. Shah, A.R., Murthy, P.L., Mital, S.K.& Bhatt, R.T. "Probabilisitc Modeling of Ceramic Matrix Composite Strength." Journal of Composite Materials. 34 (2000): 670-688.
2. Murthy, P.L., Mital, S.K., Shah, A.R. "Probabilistic Micromechanics and Macromechanics for Ceramic Matrix Composites." NASA/TM 1997-4766. 1997.
3. DiCarlo, J.A., Yun, H.M., Morscher, G.N., Bhatt, R.T. "SiC/Sic Composites for 1200 Degrees Farenheit and Above." NASA/TM 2004-213048. 2004.
4. Kwon, Y.W. & Altekin, A. "Multilevel, Micro/Macro-Approach for Analysis of Woven-Fabric Composite Plates." Journal of Composite Materials. 36 (2001): 1005-1022.
5. Goldberg, R.K., Bonacuse, P.J., Mital, S.K., Calomin, A.C. "High Fidelity Meso-scale Modeling for CMC Life Prediction." NASA Fundamental Aeronautics Program Technical Conference. Cleveland, OH, 2011.
6. Morscher, G.N. "Modeling the Elastic Modulus of 2D Woven SiC Composites." Composites Science and Technology. 66 (2006): 2804-2814.
7. Whitcomb, J. & Tang, X. "Effective Moduli of Woven Composites." Journal of Composite Materials. 35 (2000): 2127-2144.
8. Smarslok, B., Haftka, R. & Ifju, P. "A Correlation Model for Graphite/Epoxy Properties for Propgating Uncertainty in Strain Response." 23rd Technical Conference of the American Society for Composites. Memphis, TN, 2008.
9. Marrey, R.V. & Sankar, B.V. "Analytical Method for Micromechanics of Textile Composites." Composites Science and Technology. 57 (1997): 703-713.
10. Bonacuse, P.J., Goldberg, R.K., Mital, S.K. "Characterization of the As-Manufactured Variability in a CVI SiC/SiC Woven Composite." ASME Turnbo Expo. Vancouver, BC, Canada, 2011
11. Reid, A. et.al. "Modeling Microstructures with OOF2." Int. J. Materials and Product Technology 35 (2009): 361-373.
12. "ABAQUS version 6.9." http://www.simulia.com/products/abaqus_fea.html.
13. Mital, S.K., Goldberg, R.K., & Bonacuse, P.J. "Two-Dimensional Nonlinear Finite Element Analysis of CMC Microstructures." ASME Turbo Expo. Vancouver, BC, Canada, 2011.
14. R.V. Marrey and B.V. Sankar (1995) "Micromechanical Models for Textile Structural Composites", NASA Contractor Report 198229.
15. Huang, H. & Talreja, R. "Effects of void geometry on elastic properties of unidirectional fiber reinforced composites." Composites Science and Technology. 65 (2005): 1964-1981.
16. Viana, F. SURROGATES Toolbox User's Guide, Version 2.1, http://sites.google.com/site/felipeacviana/surrogatestoolbox, 2010.